

Description of Deconfinement at Finite Matter Density in a Generalized Nambu–Jona-Lasinio Model

Hu Li and C.M. Shakin*

Department of Physics and Center for Nuclear Theory

Brooklyn College of the City University of New York

Brooklyn, New York 11210

(Dated: June, 2002)

arXiv:hep-ph/0207135v1 10 Jul 2002

Abstract

Recent years have seen extensive applications of the Nambu–Jona-Lasinio (NJL) model in the study of matter at high density. There is a good deal of interest in the predictions of diquark condensation and color superconductivity, with suggested applications to the study the properties of neutron stars. As the researchers in this field note, the NJL model does not describe confinement, so that one is limited to the study of the deconfined phase, which may set in at several times nuclear matter density. Recently, we have extended the NJL model to include a covariant confinement model. Our model may be used to study the properties of the full range of light mesons, including their radial excitations, in the 1-3 GeV energy domain. Most recently we have used our extended model to provide an excellent fit to the properties of the $\eta(547)$ and $\eta'(958)$ mesons and their radial excitations. The mixing angles and decay constants are given successfully in our model. In the present work our goal is to include a phenomenological model of deconfinement at finite matter density, using some analogy to what is known concerning “string breaking” and deconfinement at finite temperature. Various models may be used, but for this work we choose a specific model for the density dependence of the parameters of our confining interaction. We perform relativistic random-phase-approximation (RPA) calculations of the properties of the $\pi(138)$, $K(495)$, $f_0(980)$, $a_0(980)$ and $K_0^*(1430)$ mesons and their radial excitations. In the model chosen for this work, there are no mesonic states beyond about $2\rho_{NM}$, where ρ_{NM} is the density of nuclear matter. (The density for deconfinement in our model may be moved to higher values by the change of one of the parameters of the model.) This inability of the model to support hadronic excitations at large values of the density is taken as a signal of deconfinement. In addition to the density dependence of the confining interaction, we use the density-dependent quark mass values obtained in either the SU(2) or SU(3)-flavor versions of the NJL model. We stress that other assumptions for the density dependence of the confinement potential, other than that used in this work, maybe considered in future work, particularly if we are able to obtain further insight in the dynamics of deconfinement at finite matter density.

PACS numbers: 12.39.Fe, 12.38.Aw, 14.65.Bt

*email:casbc@cunyvm.cuny.edu

I. INTRODUCTION

In recent years we have developed a generalized Nambu–Jona-Lasinio (NJL) model that incorporates a covariant model of confinement [1-5]. The Lagrangian of the model is

$$\begin{aligned}
 \mathcal{L} = & \bar{q}(i\not{\partial} - m^0)q + \frac{G_S}{2} \sum_{i=0}^8 [(\bar{q}\lambda^i q)^2 + (\bar{q}i\gamma_5\lambda^i q)^2] \\
 & - \frac{G_V}{2} \sum_{i=0}^8 [(\bar{q}\lambda^i\gamma_\mu q)^2 + (\bar{q}\lambda^i\gamma_5\gamma_\mu q)^2] \\
 & + \frac{G_D}{2} \{\det[\bar{q}(1 + \gamma_5)q] + \det[\bar{q}(1 - \gamma_5)q]\} \\
 & + \mathcal{L}_{conf}, \tag{1.1}
 \end{aligned}$$

where the $\lambda^i (i = 0, \dots, 8)$ are the Gell-Mann matrices, with $\lambda^0 = \sqrt{2/3}\mathbf{1}$, $m^0 = \text{diag}(m_u^0, m_d^0, m_s^0)$ is a matrix of current quark masses and \mathcal{L}_{conf} denotes our model of confinement. Many applications have been made in the study of light meson spectra, decay constants, and mixing angles. In the present work we extend our model to include a description of deconfinement at finite density.

There has been extensive application of the NJL model in the study of matter at high density, with particular interest in diquark condensation and color superconductivity [6-9]. These studies find application in the study of neutron stars. The NJL model is the model of choice, since little insight into the properties of matter at finite density can be obtained in lattice simulations of QCD. This problem is associated with the introduction of a chemical potential, which makes the Euclidean-space fermion determinant complex.

The use of the NJL model in the hadronic phase of matter is limited, since the standard version of the model does not contain a model of confinement [10-12]. It is clearly of value to extend the NJL model so that one can study the full range of densities of interest at this point in time. We are encouraged in this program by recent results, obtained in lattice simulations of QCD with dynamical quarks, that provide information on the temperature dependence of the confining interaction [13]. It is generally believed that the presence of matter will play a role similar to that of finite temperature, with deconfinement taking place at some finite density, which might be several times that of nuclear matter. In the present work we make a specific assumption concerning the density dependence of the confining field and then calculate meson spectra in the presence of our density-dependent confining interaction. We also take into account the density dependence of the constituent quark

masses, which is calculated in the SU(2) or SU(3)-flavor version of the NJL model. As is well known, the presence of matter leads to a reduction in the magnitude of the quark vacuum condensates, which represents a partial restoration of chiral symmetry in matter.

Our calculations of the properties of mesons in matter is made using a covariant random-phase-approximation (RPA) formalism, which we have developed for the study of mesons in vacuum [1-5]. The organization of our work is as follows. In Section II we provide a short review of our treatment of Lorentz-vector confinement in our generalized NJL model. In Section III we describe the variation of the up, down and strange quark constituent quark masses in matter. In Section IV we discuss some recent work concerning the temperature dependence of the confining interaction, as obtained in lattice simulations of QCD with dynamical quarks. We also specify the density dependence of the confining field that we use in this work in Section IV. In Section V we comment upon the phenomenon of pion condensation. (In our work we introduce a small density dependence of the coupling constants of the NJL model to simulate effects that prevent the formation of a pion condensate in nuclear matter.) In Section VI we discuss our covariant RPA calculations of meson properties in vacuum and indicate how these calculations are modified in matter. Results of our RPA calculations of the properties of pseudoscalar mesons in matter are presented in Section VII, while Section VIII contains similar results for scalar mesons. In the case of scalar mesons, we study the $a_0(980)$, $f_0(980)$, and $K_0^*(1430)$ mesons and their radial excitations. Finally, Section IX contains some further discussion and conclusions.

II. MODELS OF CONFINEMENT

There are several models of confinement in use. One approach is particularly suited to Euclidean-space calculations of hadron properties. In that case one constructs a model of the quark propagator by solving the Schwinger-Dyson equation. By appropriate choice of the interaction one can construct a propagator that has no on-mass-shell poles when the propagator is continued into Minkowski space. Such calculations have recently been reviewed by Roberts and Schmidt [14]. In the past, we have performed calculations of the quark and gluon propagators in Euclidean space and in Minkowski space. These calculations give rise to propagators which did not have on-mass-shell poles [15-18]. However, for our studies of meson spectra, which included descriptions of radial excitations, we found it useful to work

in Minkowski space.

The construction of our covariant confinement model has been described in a number of works [1-5]. We have made use of Lorentz-vector confinement, so that the Lagrangian of our model exhibits chiral symmetry. We begin with the form $V^C(r) = \kappa r \exp[-\mu r]$ and obtain the momentum-space potential via Fourier transformation. Thus,

$$V^C(\vec{k} - \vec{k}') = -8\pi\kappa \left[\frac{1}{[(\vec{k} - \vec{k}')^2 + \mu^2]^2} - \frac{4\mu^2}{[(\vec{k} - \vec{k}')^2 + \mu^2]^3} \right], \quad (2.1)$$

with the matrix form

$$\bar{V}^C(\vec{k} - \vec{k}') = \gamma^\mu(1)V^C(\vec{k} - \vec{k}')\gamma_\mu(2), \quad (2.2)$$

appropriate to Lorentz-vector confinement. The potential of Eq. (2.1) is used in the meson rest frame. We may write a covariant version of $V^C(\vec{k} - \vec{k}')$ by introducing the four-vectors

$$\hat{k}^\mu = k^\mu - \frac{(k \cdot P)P^\mu}{P^2}, \quad (2.3)$$

and

$$\hat{k}'^\mu = k'^\mu - \frac{(k' \cdot P)P^\mu}{P^2}. \quad (2.4)$$

Thus, we have

$$V^C(\hat{k} - \hat{k}') = -8\pi\kappa \left[\frac{1}{[-(\hat{k} - \hat{k}')^2 + \mu^2]^2} - \frac{4\mu^2}{[-(\hat{k} - \hat{k}')^2 + \mu^2]^3} \right]. \quad (2.5)$$

Originally, the parameter $\mu = 0.010$ GeV was introduced to simplify our momentum-space calculations. However, in the light of the following discussion, we can remark that μ may be interpreted as describing screening effects as they affect the confining potential [13].

In our work, we found that the use of $\kappa = 0.055$ GeV² gave very good results for meson spectra. Here, κ for the Lorentz-vector potential is about one-fourth of the value of κ for Lorentz-scalar confinement. This difference arises since the Dirac matrices $\gamma^\mu(1)\gamma_\mu(2)$ in Eq. (2.2) give rise to a factor of 4 upon forming various Dirac trace operations, so that the *effective* value of the string tension is about the same in both Lorentz-scalar and Lorentz-vector models of confinement.

The potential $V^C(r) = \kappa r \exp[-\mu r]$ has a maximum at $r = 1/\mu$, at which point the value is $V_{max} = \kappa/\mu e = 2.023$ GeV. If we consider pseudoscalar mesons, which have $L = 0$, the

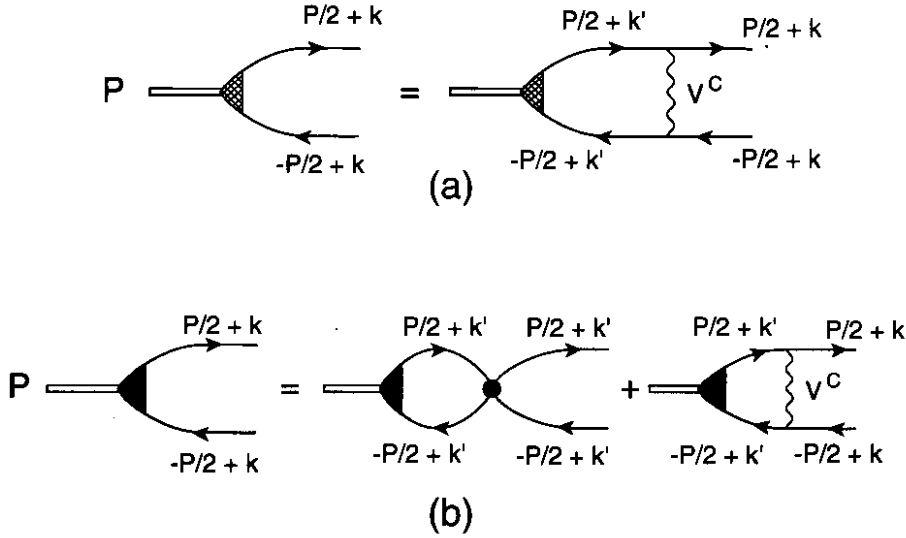


FIG. 1: a) Bound states in the confining field (wavy line) may be found by solving the equation for the vertex shown in this figure, b) Effects of both the confining field and the short-range NJL interaction (filled circle) are included when solving for the vertex shown in this figure.

continuum of the model starts at $E_{cont} = m_1 + m_2 + V_{max}$, so that for $m_1 = m_2 = m_u = m_d = 0.364$ GeV, $E_{cont} = 2.751$ GeV. It is also worth noting that the potential goes to zero for very large r . Thus, there are scattering states whose lowest energy would be $m_1 + m_2$. However, barrier penetration plays no role in our work. The bound states in the interior of the potential do not communicate with these scattering states to any significant degree. It is not difficult to construct a computer program that picks out the bound states from all the states found upon diagonalizing the random-phase-approximation Hamiltonian.

Bound states in the confining field may be found by solving the equation for the mesonic vertex function shown in Fig. 1a. Inclusion of the short-range NJL interaction leads to an equation for the vertex shown in Fig. 1b. We will return to a consideration of Fig. 1b when we discuss our covariant RPA formalism in Section VI.

III. CALCULATION OF CONSTITUENT QUARK MASS VALUES

In this Section we report upon our calculation of the density dependence of the constituent quark masses of the up (or down) and strange quarks. The role of confinement in the

calculation of the constituent mass was studied in an earlier work in which calculations were made in Euclidean space [19]. The results were similar to those obtained in Minkowski-space calculations in which confinement was neglected and it is the latter calculations which we discuss here.

The equations for the quark masses in the SU(3)-flavor NJL model are [11]

$$m_u = m_u^0 - 2G_S \langle \bar{u}u \rangle - G_D \langle \bar{d}d \rangle \langle \bar{s}s \rangle, \quad (3.1)$$

$$m_d = m_d^0 - 2G_S \langle \bar{d}d \rangle - G_D \langle \bar{u}u \rangle \langle \bar{s}s \rangle, \quad (3.2)$$

$$m_s = m_s^0 - 2G_S \langle \bar{s}s \rangle - G_D \langle \bar{u}u \rangle \langle \bar{d}d \rangle, \quad (3.3)$$

where $\langle \bar{u}u \rangle$, $\langle \bar{d}d \rangle$ and $\langle \bar{s}s \rangle$ are the quark vacuum condensates. For example, with $N_c = 3$,

$$\langle \bar{u}u \rangle = -4N_c i \int \frac{d^4k}{(2\pi)^4} \frac{m_u}{k^2 - m_u^2 + i\epsilon}. \quad (3.4)$$

If this integral is evaluated in a Minkowski-space calculation, a cutoff is used such that $|\vec{k}| \leq \Lambda_3$. Thus,

$$\langle \bar{u}u \rangle = -4N_c \int^{\Lambda_3} \frac{d^3k}{(2\pi)^3} \frac{m_u}{2E_u(\vec{k})}, \quad (3.5)$$

etc. Here $E_u(\vec{k}) = [\vec{k}^2 + m_u^2]^{1/2}$.

For studies at finite density, we consider the presence of two Fermi seas of up and down quarks with Fermi momentum k_F . We also take $m_u^0 = m_d^0$ and obtain the density-dependent equations, with $\langle \bar{u}u \rangle_\rho = \langle \bar{d}d \rangle_\rho$,

$$m_u(\rho) = m_u^0 - 2G_S \langle \bar{u}u \rangle_\rho - G_D \langle \bar{d}d \rangle_\rho \langle \bar{s}s \rangle_\rho, \quad (3.6)$$

$$m_s(\rho) = m_s^0 - 2G_S \langle \bar{s}s \rangle_\rho - G_D \langle \bar{u}u \rangle_\rho \langle \bar{d}d \rangle_\rho. \quad (3.7)$$

Equation (3.5) is now replaced by

$$\langle \bar{u}u \rangle_\rho = -4N_c \left[\int_0^{\Lambda_3} \frac{d^3k}{(2\pi)^3} \frac{m_u(\rho)}{2E_u(\vec{k})} - \int_0^{k_F} \frac{d^3k}{(2\pi)^3} \frac{m_u(\rho)}{2E_u(\vec{k})} \right], \quad (3.8)$$

with $E_u(\vec{k}) = [\vec{k}^2 + m_u^2(\rho)]^{1/2}$. On the other hand, since we do not consider a background of strange matter, we have

$$\langle \bar{s}s \rangle_\rho = -4N_c \int_0^{\Lambda_3} \frac{d^3k}{(2\pi)^3} \frac{m_s(\rho)}{2E_s(\vec{k})}, \quad (3.9)$$

with $E_s(\vec{k}) = \left[\vec{k}^2 + m_s^2(\rho) \right]^{1/2}$.

We may argue that, with respect to our mean-field analysis, the Fermi seas of up and down quarks yield contributions to the scalar density that are similar to what would be obtained if the quarks are organized into nucleons. One part of the argument is based upon the well-known model-independent relation for the density dependence of the condensate [20]

$$\frac{\langle \bar{q}q \rangle_\rho}{\langle \bar{q}q \rangle_0} = \left(1 - \frac{\sigma_N \rho}{f_\pi^2 m_\pi^2} + \dots \right), \quad (3.10)$$

where σ_N is the pion-nucleon sigma term and ρ is the density of the matter. If we take $f_\pi = 0.0942$ GeV, $m_\pi = 0.138$ GeV, $\rho_{NM} = (0.109 \text{ GeV})^3$ and $\sigma_N = 0.050$ GeV, we find a reduction of the condensate in nuclear matter of 38%, which is consistent with relativistic models of nuclear matter [21, 22].

We now consider the corresponding relation for a quark gas of up and down quarks,

$$\frac{\langle \bar{q}q \rangle_\rho}{\langle \bar{q}q \rangle_0} = \left(1 - \frac{\sigma_q \rho_q}{f_\pi^2 m_\pi^2} + \dots \right), \quad (3.11)$$

where ρ_q is the density of quarks ($\rho_q = 3\rho$) and σ_q is a ‘‘quark sigma term’’. We have shown in earlier work [23] that σ_q is in the range of 15-17 MeV, so that Eq. (3.10) and (3.11) imply that quite similar mean fields are generated by the quark gas and by nuclear matter.

In Table I and in Fig. 2, we show the results obtained when Eqs. (3.8) and (3.9) are solved with $G_S = 9.00 \text{ GeV}^{-2}$, $G_D = -240 \text{ GeV}^{-5}$, $\Lambda_3 = 0.631 \text{ GeV}$, $m_u^0 = 0.0055 \text{ GeV}$ and $m_s^0 = 0.130 \text{ GeV}$. We note that the dependence of $m_u(\rho)$ on density is approximately linear for $\rho/\rho_{NM} \leq 2$, with a 32% reduction in the value of $m_u(\rho)$ when $\rho/\rho_{NM} = 1$. Another point to note is that $m_s(\rho)$ is density-dependent for finite values of G_D , since the $\langle \bar{s}s \rangle$ condensate is modified by the coupling to the up and down quark condensates via the 't Hooft interaction. This coupling becomes less important as the up and down quark condensates are reduced at increasing density. [See Fig. 2.]

We have also considered the solution for the SU(2) version of the above equations

$$m_u(\rho) = m_u^0 - 2G_S \langle \bar{u}u \rangle_\rho, \quad (3.12)$$

and have used the parameters specified in the Klevansky review article [10], $G_S = 10.15 \text{ GeV}^{-2}$, $m_u^0 = 0.0055 \text{ GeV}$ and $\Lambda_3 = 0.631 \text{ GeV}$. The results for $m_u(\rho)$ are similar to that seen in Fig. 2, except that $m_u(0) = 0.336 \text{ GeV}$. [See Fig. 3.] In this case, $m_u(\rho)$ is reduced by about 32% when $\rho = \rho_{NM}$.

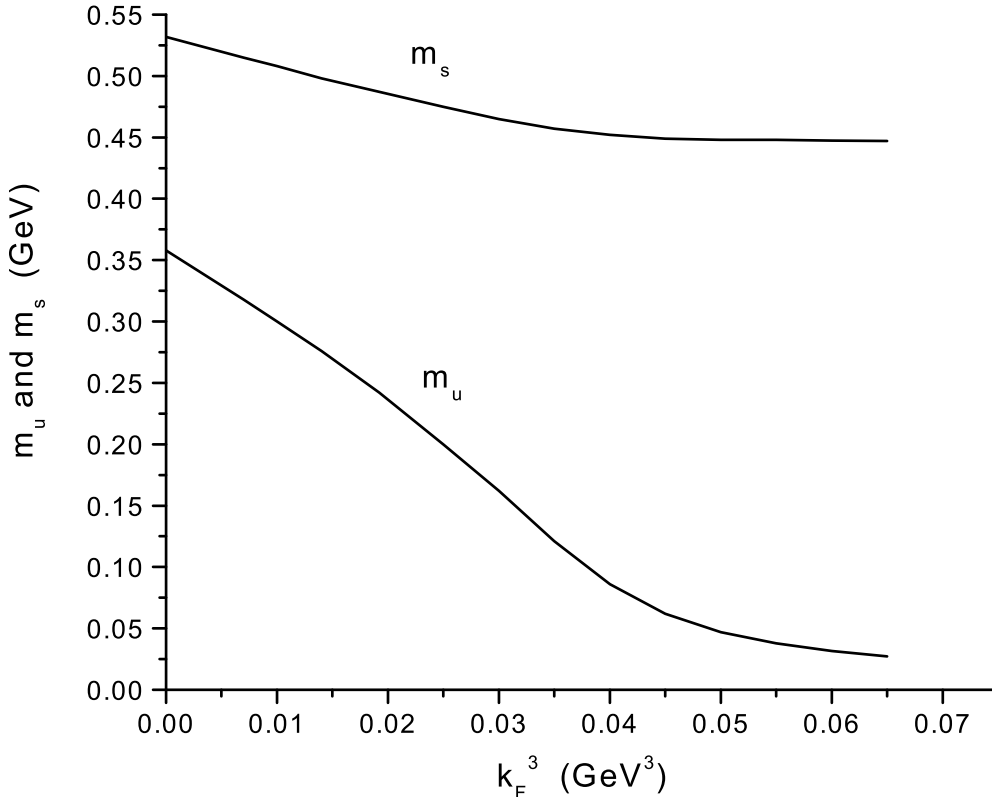


FIG. 2: The solution of Eqs. (3.6) and (3.7) for the density-dependent constituent quark masses, $m_u(\rho) = m_d(\rho)$ and $m_s(\rho)$ are shown. Here $G_S = 9.00 \text{ GeV}^{-2}$, $G_D = -240.0 \text{ GeV}^{-5}$, $\Lambda_3 = 0.631 \text{ GeV}$, $m_u^0 = 0.0055 \text{ GeV}$ and $m_s^0 = 0.130 \text{ GeV}$.

IV. DENSITY AND TEMPERATURE DEPENDENCE OF THE CONFINING FIELD

In part, our study has been stimulated by the results presented in Ref. [13] for the temperature-dependent potential, $V(r)$, in the case dynamical quarks are present. We reproduce some of the results of that work in Fig. 4. There, the filled symbols represent the results for $T/T_c = 0.68, 0.80, 0.88$ and 0.94 when dynamical quarks are present. This figure represents definite evidence of “string breaking”, since the force between the quarks appears to approach zero for $r > 1 \text{ fm}$. This is not evidence for deconfinement, which is found for $T = T_c$. Rather, it represents the creation of a second $\bar{q}q$ pair, so that one has two mesons after string breaking. Some clear evidence for string breaking at zero temperature and finite

k_F^3 (GeV ³)	ρ/ρ_{NM}	$m_u(\rho)$ [GeV]	$m_s(\rho)$ [GeV]
0.00	0.00	0.358	0.532
0.007	0.364	0.318	0.515
0.010	0.521	0.300	0.508
0.0140	0.729	0.276	0.498
0.0192	1.00	0.242	0.487
0.025	1.302	0.200	0.475
0.030	1.562	0.162	0.465
0.035	1.823	0.121	0.457
0.040	2.083	0.0860	0.452
0.045	2.343	0.0618	0.449
0.050	2.604	0.0470	0.448
0.055	2.864	0.0378	0.448
0.060	3.125	0.0316	0.448
0.065	3.385	0.0272	0.447

TABLE I: Values of $m_u(\rho)$ and $m_s(\rho)$ obtained from the solution of Eqs. (3.6) and (3.7) are given for various values of the ratio ρ/ρ_{NM} . (Here, $k_F^3 = 0.0192$ GeV³ for nuclear matter, $m_u^0 = 0.0055$ GeV, $m_s^0 = 0.130$ GeV, $\Lambda_3 = 0.631$ GeV, $G_S = 9.00$ GeV⁻², $G_D = -240.0$ GeV⁻⁵.)

density is reported in Ref. [24].

In order to study deconfinement in our generalized NJL model, we need to specify the interquark potential at finite density. We start with our model that was described in Section II. In that case we had $V^C(r) = \kappa r \exp[-\mu r]$. For the model we study in this work, we write

$$V^C(r, \rho) = \kappa r \exp[-\mu(\rho)r] \quad (4.1)$$

and put

$$\mu(\rho) = \frac{\mu_0}{1 - \left(\frac{\rho}{\rho_C}\right)^2}, \quad (4.2)$$

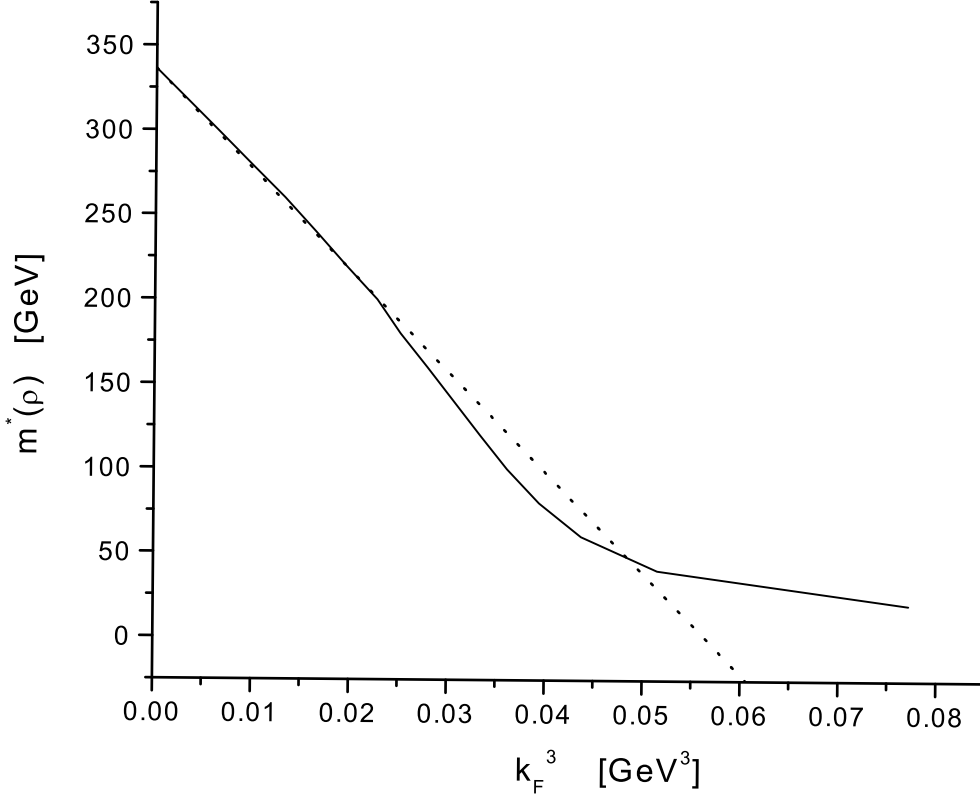


FIG. 3: The solution of Eq. (3.12) for $m_u(\rho)$ is shown. Here $G_S = 10.15 \text{ GeV}^{-2}$, $m_u^0 = 0.0055 \text{ GeV}$ and $\Lambda_3 = 0.631 \text{ GeV}$. (See Table V of Ref. [10].) The dashed line is a linear approximation to the result which we use for $\rho \leq 2\rho_{NM}$. (Nuclear matter density corresponds to $k_F^3 = 0.0192 \text{ GeV}^3$.)

with $\rho_C = 2.25\rho_{NM}$ and $\mu_0 = 0.010 \text{ GeV}$. With this modification our results for meson spectra in the vacuum are unchanged. Other forms than that given in Eqs. (4.1) and (4.2) may be used. However, in this work we limit our analysis to the model presented in these equations. The corresponding potentials for our model of Lorentz-vector confinement are shown in Fig. 5 for several values of ρ/ρ_{NM} .

We can see from Fig. 4 that, for $T = 0.94T_c$, the use of dynamical quarks leads to an approximately constant value of $V(r) = 1000 \text{ MeV}$ for larger r . If we perform a Fierz rearrangement of the Lorentz-scalar potential to study pseudoscalar $q\bar{q}$ states, one introduces a factor of 1/4, making the value at large r to be about 250 MeV. (See Eq. (B1) of Ref. [10].) However, rearranging the Lorentz-vector potential to study pseudoscalar $q\bar{q}$ states introduces

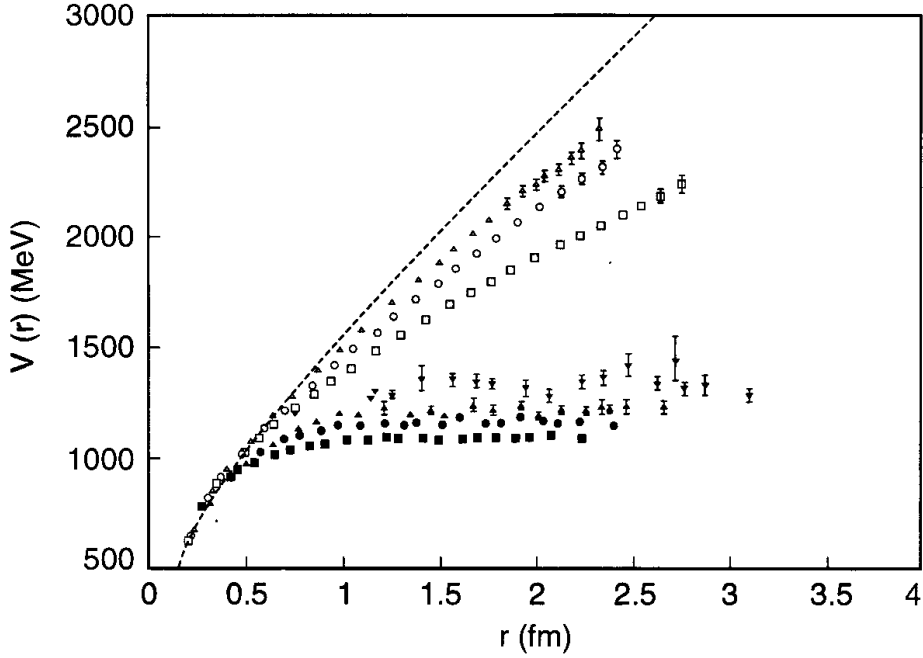


FIG. 4: A comparison of quenched (open symbols) and unquenched results (filled symbols) for the interquark potential at finite temperature [13]. The dotted line is the zero temperature quenched potential. Here, the symbols for $T = 0.80T_c$ [open triangle], $T = 0.88T_c$ [open circle], $T = 0.80T_c$ [open square], represent the quenched results. The results with dynamical fermions are given at $T = 0.68T_c$ [solid downward-pointing triangle], $T = 0.80T_c$ [solid upward-pointing triangle], $T = 0.88T_c$ [solid circle], and $T = 0.94T_c$ [solid square].

a factor of 1. Now, let us consider $\rho/\rho_{NM} = 0.94(\rho_C/\rho_{NM}) \simeq 2.11$, and find the maximum of our Lorentz-vector potential at that density from the relation $V_{max} = \kappa/\mu(\rho)e$. Using our value for $\mu(\rho)$ at $\rho/\rho_{NM} = 2.11$, we obtain $V_{max} = 0.227$ GeV. The value for the Lorentz-vector potential compares favorably with the value of $V(r)$, for large r , quoted above. This result suggests that, if the dynamics of chiral symmetry restoration and deconfinement at finite temperature is somewhat analogous to the deconfinement process at finite density, our use of $\rho/\rho_{NM} = 2.25$ may be a satisfactory choice.

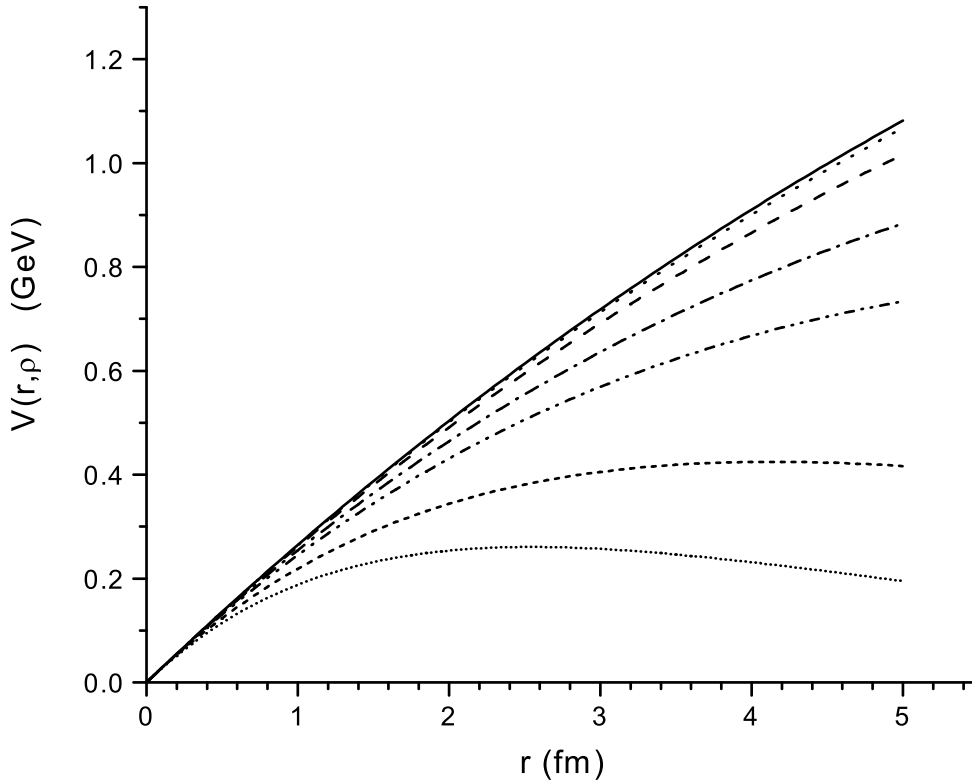


FIG. 5: Values of $V(r, \rho)$ are shown, where $V(r, \rho) = \kappa r \exp[-\mu(\rho)r]$ and $\mu(\rho) = \mu_0/[1 - (\rho/\rho_C)^2]$. Here $\rho_C = 2.25\rho_{NM}$ and $\mu_0 = 0.010$ GeV. The values of ρ/ρ_{NM} are 0.0 [solid line], 0.50 [dotted line], 1.0 [dash line], 1.50 [dash-dot line], 1.75 [dash-dot-dot line], 2.0 [short-dash line], and 2.1 [small dot line].

V. PION CONDENSATION AND THE CHOICE OF THE PARAMETERS OF THE INTERACTION

It was suggested many years ago that the ground state of nuclear matter might have an unusual structure due to presence of pionlike excitations [25]. In finite nuclei such effects could imply anomalous behavior in states with $J^\pi = 0^-, 1^+, 2^- \dots$, etc. However, the nucleon-nucleon interaction is sufficiently repulsive in the relevant channel so that pion condensation does not take place at normal nuclear matter densities. That matter has been discussed in Ref. [26]. A constant g' parametrizes the strength of a nuclear force in the spin-isospin channel that represents short-range correlation effects and exchange effects. (See Eq. (5.11a) of Ref. [26].) The phenomenological value of g' , obtained from the study of nuclear excitations, is sufficiently large so that pion condensation does not take place until about

three times nuclear matter density. (See Fig. 5.9 of Ref. [26].)

In our work we will model the effects that prevent pion condensation by introducing a density-dependent interaction for the pionic states calculated in the NJL model. We write

$$G_\pi(\rho) = G_\pi(0)[1 - 0.087\rho/\rho_{NM}], \quad (5.1)$$

where the second term in Eq. (5.1) represents medium effects that reduce the pion self-energy in matter. Here $G_\pi(0)$ is the linear combination of G_S and G_D given on page 269 of Ref. [12],

$$G_\pi = G_S + \frac{G_D}{2}\langle\bar{s}s\rangle. \quad (5.2)$$

Equation (5.1) represents our scheme for parametrizing the nuclear matter effects that prevent pion condensation. In our calculations of pionlike excitations we put $G_\pi(0) = 13.49$ GeV⁻², and used a constant values of $G_V = 11.46$ GeV⁻². We may check that our choice of $G_\pi(0)$ is reasonable by using Eq. (5.2) with $G_S = 11.84$ GeV⁻² and -180 GeV⁻⁵ $\leq G_D \leq 240$ GeV⁻⁵. These values of G_S and G_D were obtained in our extensive study of the eta mesons [1]. Thus, if we take $\langle\bar{s}s\rangle = -(0.258 \text{ GeV})^3$ and $G_D = -190$ GeV⁻⁵, we find $G_\pi(0) = 13.47$ GeV⁻². This analysis suggests that, once we fix our parameters in the study of the eta mesons, we can then infer the parameters needed for our study of the pion in vacuum.

For this work, in our study of the kaon, we use $G_K(0) = 13.07$ GeV⁻² and $G_V = 11.46$ GeV⁻². Note that [12]

$$G_K(0) = G_S + \frac{G_D}{2}\langle\bar{d}d\rangle_0. \quad (5.3)$$

If we take $G_S = 11.84$ GeV⁻², $G_D = -190$ GeV⁻⁵ and $\langle\bar{u}u\rangle = -(0.240 \text{ GeV})^3$, we find $G_K(0) = 13.15$ GeV⁻², which is close to the value of $G_K(0) = 13.07$ GeV⁻² used in our calculations. In our work we have used

$$G_K(\rho) = G_K(0)[1 - 0.087\rho/\rho_{NM}]. \quad (5.4)$$

In the case of the kaon, about 40% of the assumed density dependence of $G_K(\rho)$ may be attributed to the density dependence of $\langle\bar{u}u\rangle_\rho$ or $\langle\bar{d}d\rangle_\rho$. We may consider the relation

$$G_K(\rho) = G_S(\rho) + \frac{G_D}{2}\langle\bar{d}d\rangle_\rho, \quad (5.5)$$

and use a somewhat smaller reduction of $G_S(\rho)$ for the kaon than that used for the pion in Eq. (5.5), since the reduction of $\langle\bar{u}u\rangle_\rho$ or $\langle\bar{d}d\rangle_\rho$ in matter effectively reduces the interaction strength.

In the absence of $a_0 - f_0$ coupling we have $G_{33}^S = G_{a_0} = G_S - (G_D/2)\langle\bar{s}s\rangle$ [12]. If we again put $G_S = 11.84 \text{ GeV}^{-2}$, $G_D = -190 \text{ GeV}^{-5}$, and $\langle\bar{s}s\rangle = -(0.258 \text{ GeV})^3$, we have $G_{a_0} = 10.21 \text{ GeV}^{-2}$, which places the $a_0(980)$ at 1.13 GeV. However, in the case of the scalar mesons there exist significant contributions to the interaction from processes that describe the scalar meson decay to two-meson channels. An extended discussion of these effects was given in an early work on scalar mesons [27]. In the case of the $f_0(980)$ we presented a discussion of such terms as they affect the energy predicted for the $f_0(980)$ in Ref. [28].

In order to take into account these effects, which are not included in our RPA calculations, we increase the value of the a_0 coupling constant to $G_{a_0} = 13.10 \text{ GeV}^{-2}$. That has the effect of moving the $a_0(980)$ mass down to 980 MeV.

We also introduce some density dependence of the interaction to avoid an “ a_0 condensate”, which would otherwise take place at $\rho = 1.75\rho_{NM}$, if we use $m_u(\rho) = m_d(\rho) = 0.0055 + 0.3585(1 - 0.4\rho/\rho_{NM})$. Thus, we use $G_{a_0}(\rho) = G_{a_0}(0)[1 - 0.045\rho/\rho_{NM}]$ when we allow for the rapid decrease in the value of $m_u(\rho) = m_d(\rho)$ given by the above expression. It is possible that the small reduction of $G_{a_0}(\rho)$ in matter given above has its origin in a somewhat smaller attraction generated at the larger densities by the real part of the polarization operator that describes decay to the two-meson channels [27, 28]. We will provide further details of our treatment of the scalar mesons in Section VIII.

VI. RANDOM PHASE APPROXIMATION FOR MESONIC EXCITATIONS

In this work we report upon covariant random-phase-approximation (RPA) calculations of meson spectra in vacuum and in dense matter. Before writing the equations of our model, it is worth discussing some properties of RPA calculations made for many-body systems [29, 30]. For example, such calculations have been performed to study excited states of nuclei. In the RPA one usually does not attempt to construct the wave function of the ground state. Rather, one considers amplitudes of particle-hole operators taken between the excited state and the ground state. The dominant amplitude usually involves the creation of a hole in the ground state and the creation of a particle in what are predominantly unoccupied

states. Smaller amplitudes are found if one destroys a hole in the ground state and destroys a particle in the predominantly unoccupied states. These smaller amplitudes are only nonzero, if one allows for correlations in the ground state.

Such RPA calculations are particularly important for states that are collective with respect to matrix elements of electromagnetic transition operators, for example. In hadron physics the most “collective state” is the $\pi(138)$. In this case the “large” and “small” components of the wave function, in the sense of the RPA, are comparable in magnitude and approach equality in magnitude as one approaches the chiral limit, when $m_\pi \rightarrow 0$.

Another important feature of RPA calculations is that they may be considered as an investigation of the properties of small oscillations about the ground state. Thus, if one obtains an imaginary energy value for the ground state, one infers that the ground state is unstable. A new ground state must be constructed that will yield real eigenvalues. (Note that imaginary eigenvalues may be obtained, since the RPA Hamiltonian is not Hermitian.)

There is a strong analogy that can be made between the particle-hole RPA calculations described above and the calculation of mesonic excitations. For example, a “hole” in the ground state (the vacuum) is an antiquark, while the particle state is the quark. If we perform relativistic RPA calculations for the pion and its radial excitations, an imaginary energy calculated for the pion is a signal of pion condensation.

Random-phase-approximation equations may be derived using the vertex equation of Fig. 1b. The RPA equations for the study of the pion, kaon, and eta mesons were derived in Ref. [1]. In the case of the pion and kaon we include pseudoscalar—axial-vector coupling. The most complex case is that of the eta mesons which, in addition to pseudoscalar—axial-vector coupling, involves singlet-octet coupling in the flavor sector.

In this work we only record the equations in the simplest example, that of RPA calculations for the a_0 mesons [31]. In this case the large component is denoted as $\phi^+(k)$, while the small component is $\phi^-(k)$. These functions are found to satisfy coupled equations for mesons in vacuum:

$$\begin{aligned}
2E_u(k)\phi^+(k) + \int dk' [H_C(k, k') + H_{NJL}(k, k')]\phi^+(k') \\
+ \int dk' H_{NJL}(k, k')\phi^-(k') = P^0\phi^+(k),
\end{aligned}
\tag{6.1}$$

$$\begin{aligned}
& -2E_u(k)\phi^-(k) - \int dk' [H_C(k, k') + H_{NJL}(k, k')]\phi^-(k') \\
& - \int dk' H_{NJL}(k, k')\phi^+(k') = P^0\phi^-(k),
\end{aligned} \tag{6.2}$$

where $E_u(k) = [\vec{k}^2 + m_u^2]^{1/2}$,

$$H_C(k, k') = -\frac{1}{(2\pi)^2} \frac{[2V_0^C(k, k')k^2k'^2 + kk'V_1^C(k, k')]}{E_u(k)E_u(k')}, \tag{6.3}$$

and

$$H_{NJL} = \frac{8N_c}{(2\pi)^2} \frac{k^2k'^2G_{a_0}e^{-k^2/2\alpha^2}e^{-k'^2/2\alpha^2}}{E_u(k)E_u(k')}. \tag{6.4}$$

In Eq. (6.3) we have introduced

$$V_l^C(k, k') = \frac{1}{2} \int_{-1}^1 dx P_l(x) V^C(\vec{k} - \vec{k}'). \tag{6.5}$$

Here, $x = \cos\theta$ and $P_l(x)$ is a Legendre function. The terms $\exp[-k^2/2\alpha^2]$ and $\exp[-k'^2/2\alpha^2]$ are regulators with $\alpha = 0.605$ GeV.

In order to solve these equations in the presence of matter, we replace m_u , G_{a_0} and μ_0 by $m_u(\rho)$, $G_{a_0}(\rho)$ and $\mu(\rho)$. (Recall that $\mu(\rho) = \mu_0/[1 - (\rho/\rho_C)^2]$.) In our calculation for the a_0 states we have taken $m_u(\rho) = m_u^0 + 0.3585 \text{ GeV} [1 - 0.4\rho/\rho_{NM}]$ and $G_{a_0}(\rho) = G_{a_0}(0)[1 - 0.045\rho/\rho_{NM}]$, with $m_u^0 = 0.0055$ GeV. As an alternative, the mass values for $m_u(\rho) = m_d(\rho)$ may be taken from Table I.

VII. RESULTS OF NUMERICAL CALCULATIONS: PSEUDOSCALAR MESONS

The choice of the parameters in the case of the pion and its radial excitations was discussed in Section V. We use $G_\pi(\rho) = G_\pi(0)[1 - 0.087\rho/\rho_{NM}]$ and $m_u(\rho) = m_d(\rho) = 0.0055 + 0.3585[1 - 0.4\rho/\rho_{NM}]$ with $G_\pi(0) = 13.49 \text{ GeV}^{-2}$ and $G_V = 11.46 \text{ GeV}^{-2}$. Also, $\mu(\rho) = \mu_0/[1 - (\rho/\rho_C)^2]$ with $\mu_0 = 0.010$ GeV and $\rho_C = 2.25\rho_{NM}$.

The results of our calculations are shown in Fig. 6. At $\rho = 0$, the first radial excitation of the pion is found at 1.319 GeV. The large number of states above 1.3 GeV have wave functions that are dominated by either the γ_5 or $\gamma_0\gamma_5$ vertex. The pion wave function has mainly a γ_5 vertex structure, with a small admixture of the $\gamma_0\gamma_5$ vertex. (The axial-vector part of the wave function makes a significant contribution in the calculation of the pion decay constant, f_π .)

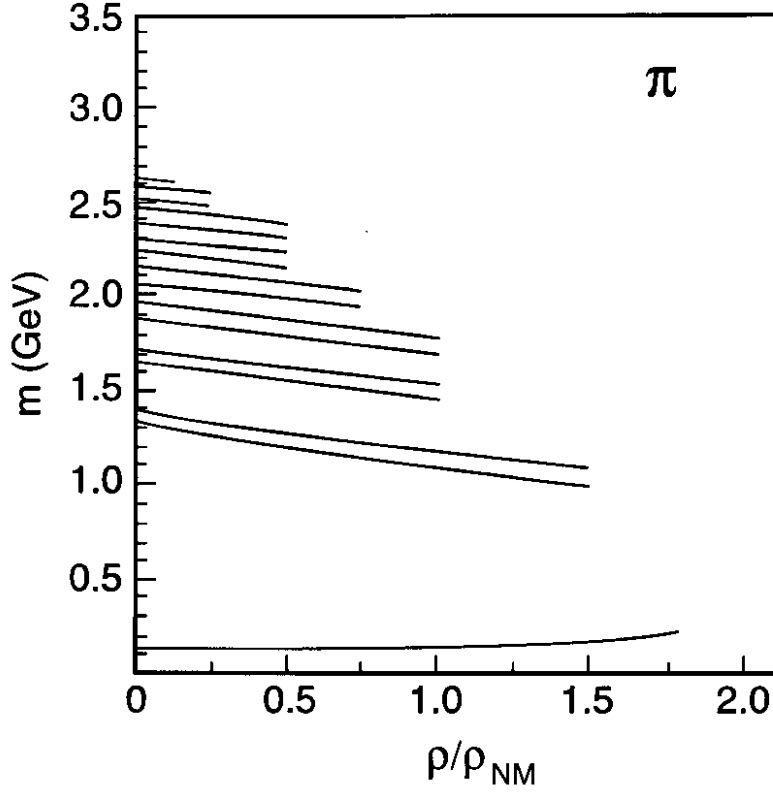


FIG. 6: The mass values for the pion and its radial excitations are presented as a function of the density of matter. Here, $G_\pi(\rho) = G_\pi(0)[1 - 0.087\rho/\rho_{NM}]$ and $m_u(\rho) = m_d(\rho) = m_u^0 + 0.3585 \text{ GeV}[1 - 0.4\rho/\rho_{NM}]$, with $m_u^0 = 0.0055 \text{ GeV}$. We use $G_\pi(0) = 13.49 \text{ GeV}^{-2}$, $G_V = 11.46 \text{ GeV}^{-2}$ and $\mu = \mu_0/[1 - (\rho/\rho_C)^2]$, with $\mu_0 = 0.010 \text{ GeV}$ and $\rho_C = 2.25\rho_{NM}$.

It may be seen from the figure, that with the reduction of the value of the constituent mass and of the confining field with increasing values of ρ/ρ_{NM} , the radial excitations that appear as bound states become fewer in number. Beyond $\rho/\rho_{NM} = 1.50$ only the nodeless pion wave function is bound and that state is no longer supported beyond $\rho/\rho_{NM} \simeq 1.80$. That represents the beginning of the deconfined phase in the case of the pion for the model introduced in this work.

Somewhat similar behavior is found for the kaon and its radial excitations, as may be seen in Fig. 7. Here we have used the mass values given in Table I and $G_K(\rho) = G_K(0)[1 - 0.087\rho/\rho_{NM}]$ with $G_K(0) = 13.07 \text{ GeV}^{-2}$ and $G_V = 11.46 \text{ GeV}^{-2}$. Again we see only a

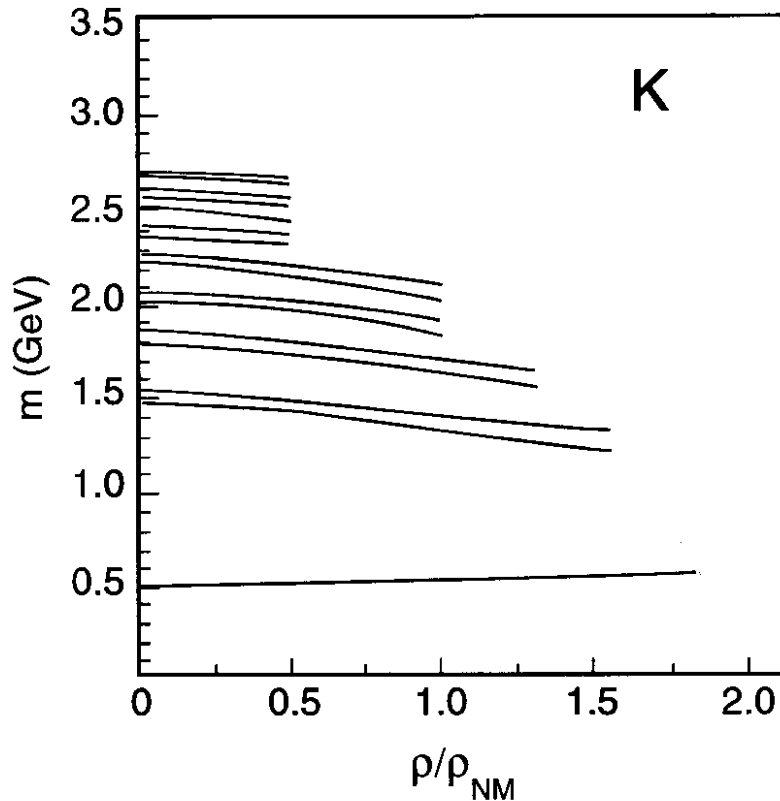


FIG. 7: Mass values of the K mesons are shown as a function of the density of matter. Here we use $G_K(0) = 13.07 \text{ GeV}^{-2}$, $G_K(\rho) = G_K(0)[1 - 0.087\rho/\rho_{NM}]$, $G_V = 11.46 \text{ GeV}^{-2}$ and $\mu = \mu_0/[1 - (\rho/\rho_C)^2]$, with $\mu_0 = 0.010 \text{ GeV}$ and $\rho_C = 2.25\rho_{NM}$. The mass values given in Table I are used.

small increase of the mass of the nodeless state, the pseudo Goldstone boson, as ρ/ρ_{NM} is increased. We again find deconfinement for $\rho/\rho_{NM} > 1.8$. The density dependence of $G_K(\rho)$ is taken to be the same as in the case of the pion. However, in this case, we have noted previously that about 40% of the reduction of $G_K(\rho)$ with increasing density may be ascribed to the density dependence of the up and down quark condensates, $\langle \bar{u}u \rangle_\rho$ and $\langle \bar{d}d \rangle_\rho$. The calculation of the density dependence of the coupling constants in our model is a major undertaking and is beyond the scope of this work.

VIII. RESULTS OF NUMERICAL CALCULATIONS: SCALAR MESONS

We have recently discussed the properties of the $f_0(980)$, giving particular attention to the role of the polarization diagrams that describe the decay of the f_0 mesons to the $\pi\pi$ or $K\bar{K}$ channels [28]. (See Fig. 2 of Ref. [28].) However, when we diagonalize the RPA Hamiltonian we do not take those terms into account. Calculations of such effects are more easily made if we construct a quark-antiquark T matrix. For a single channel example we may write

$$t(p^2) = -\frac{G}{1 - GJ(p^2)}, \quad (8.1)$$

where G is the appropriate coupling constant for that channel and $J(p^2)$ is the corresponding vacuum polarization operator. In our model $J(p^2)$ is calculated with the confining vertex function that appears in Fig. 1a as a crosshatched region. (See Fig. 1 of Ref. [28].) The resulting $J(p^2)$ is a real function, which is singular at the values of p^2 for which there is a bound state in the confining field. If we include polarization diagrams that describe coupling to two-meson decay channels, Eq. (8.1) is modified to read

$$t(p^2) = -\frac{G}{1 - G[J(p^2) + \text{Re}K(p^2) + i\text{Im}K(p^2)]}. \quad (8.2)$$

The calculation of $J(p^2)$ and $K(p^2)$ has been extensively discussed in our earlier work. In the case of the scalar mesons, inclusion of $\text{Re}K(p^2)$ can move the mass of the lowest-energy state down by about 70-100 MeV [27, 28].

In the case of the $a_0(980)$, the use of G_S and G_D determined in our study of the eta mesons places the $a_0(980)$ at 1.13 GeV. In the present work we have increased the coupling constant from $G_{a_0} = 10.21 \text{ GeV}^{-2}$ to $G_{a_0} = 13.10 \text{ GeV}^{-2}$ to move the lowest a_0 state down to 980 MeV. That creates a problem of “ a_0 condensation” which we avoid by taking $G_{a_0}(\rho) = G_{a_0}(0)[1 - 0.045\rho/\rho_{NM}]$. One may speculate that the effects that increase the effective coupling strength from $G_{a_0} = 10.21 \text{ GeV}^{-2}$ to $G_{a_0} = 13.10 \text{ GeV}^{-2}$ have some density dependence that reduces the induced attraction at the higher densities.

In Fig. 8 we show our results for the a_0 mesons. There we see deconfinement at about $\rho = 2.0\rho_{NM}$ which is a slightly larger value of the density than that found for the other mesons studied in this work. However, the behavior of the lowest a_0 state with increasing density is made somewhat uncertain because of our lack of knowledge of the appropriate form for $G_{a_0}(\rho)$.

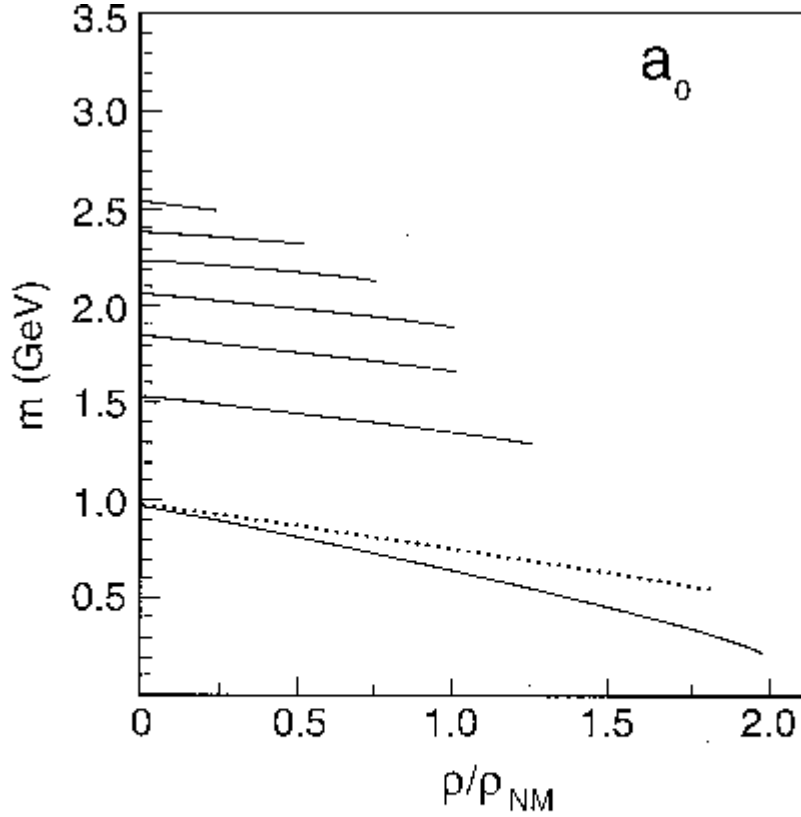


FIG. 8: Mass values for the a_0 mesons are given as a function of the matter density. Here, we have used $G_{a_0}(0) = 13.10 \text{ GeV}^{-2}$ and $G_{a_0}(\rho) = G_{a_0}(0)[1 - 0.045\rho/\rho_{NM}]$. We have used $m_u = m_u^0 + 0.3585 \text{ GeV}[1 - 0.4\rho/\rho_{NM}]$ with $m_u^0 = 0.0055 \text{ GeV}$. The dotted line results, if we put $G_{a_0}(\rho) = G_{a_0}(0)[1 - 0.087\rho/\rho_{NM}]$ and use the mass values of Table I. The dotted curve is similar to the curve for the a_0 mass given in Ref. [31]. The curves representing the masses of the radial excitations are changed very little when we use the second form for $G_{a_0}(\rho)$ given above.

For our study of the f_0 mesons we work in a singlet-octet representation and use the coupling constants $G_{00}^S = 14.25 \text{ GeV}^{-2}$, $G_{88}^S = 10.65 \text{ GeV}^{-2}$ and $G_{08}^S = G_{80}^S = 0.4953 \text{ GeV}^{-2}$. This choice yields 980 MeV for the mass of the $f_0(980)$. The fact that $G_{00}^S > G_{88}^S$ is a feature of the 't Hooft interaction and leads to the $f_0(980)$ being mainly a singlet state [28]. (For the $\eta(547)$ the behavior of the 't Hooft interaction is such that $G_{88}^S > G_{00}^S$ [12, 28] and, therefore, the $\eta(547)$ is predominantly a flavor octet meson [1].)

In our study of the f_0 mesons at finite density we use the mass values of Table I and do not introduce any density dependence for G_{00}^S , G_{88}^S and G_{08}^S . The results of our calculation

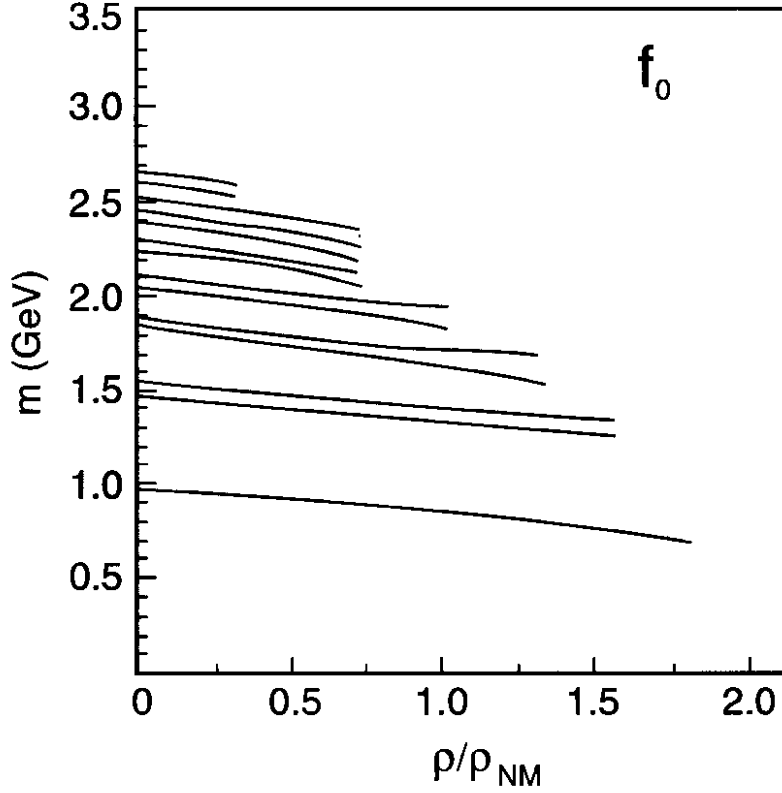


FIG. 9: The figure shows the mass values of the f_0 mesons as a function of density. The mass values for the quarks are taken from Table I. In a singlet-octet representation, we have used the constants $G_{00}^S = 14.25 \text{ GeV}^{-2}$, $G_{08}^S = 10.65 \text{ GeV}^{-2}$ and $G_{88}^S = 0.4953 \text{ GeV}^{-2}$. Deconfinement takes place somewhat above $\rho = 1.8\rho_{NM}$. Here $\mu = \mu_0/[1 - (\rho/\rho_C)^2]$ with $\mu_0 = 0.010 \text{ GeV}$ and $\rho_C = 2.25\rho_{NM}$.

are shown in Fig. 9. Since the $f_0(980)$ has a significant $\bar{s}s$ component, the mass value only decreases slowly, with a value of 700 MeV for the lowest f_0 state at $\rho/\rho_{NM} = 1.82$, where deconfinement sets in.

In Ref. [28] we provide a discussion of the T matrix for the singlet-octet channels. There the role of $K_{00}^S(p^2)$, $K_{08}^S(p^2)$ and $K_{88}^S(p^2)$ in lowering the energy predicted for the $f_0(980)$ is discussed in some detail.

Our results for the energy levels of the K_0^* mesons are given in Fig. 10. In this case we use a constant value for $G_{K_0^*} = 10.25 \text{ GeV}^{-2}$. The results are hardly modified if we allow for a small density dependence of $G_{K_0^*}$. Since the K_0^* mesons contain a strange quark, the

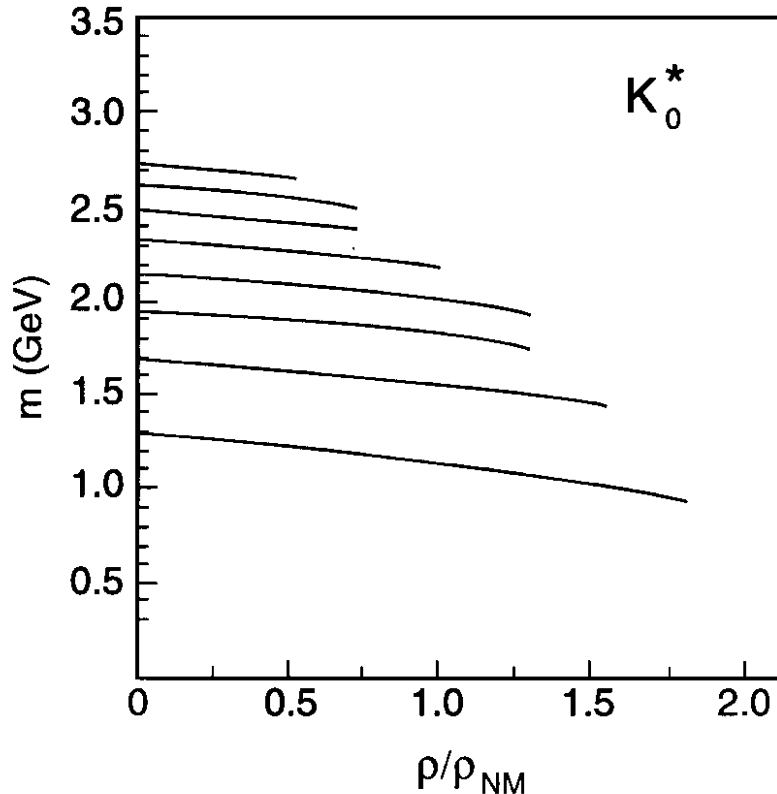


FIG. 10: The figure shows the mass values obtained for the K_0^* mesons as a function of density. Here we use a constant $G_{K_0^*} = 10.25 \text{ GeV}^{-2}$. Deconfinement takes place somewhat above $\rho = 1.8\rho_{NM}$. The quark mass values were taken from Table I.

density dependence of their energies is not as marked as that of the a_0 mesons which only contain up and down quarks in our model. In that regard, the behavior of the K_0^* mesons is more like that of the f_0 mesons, which have some strange quark content. Again we see deconfinement for $\rho > 1.8\rho_{NM}$.

IX. DISCUSSION

We originally chose $\rho_C = 2.25\rho_{NM}$, since the curve in Fig. 2 that shows the values of $m_u(\rho)$ seemed to change its behavior at about $k_F^3 = 0.045 \text{ GeV}^3$, which corresponds to $\rho \simeq 2.3\rho_{NM}$. We can attempt to see if that is a reasonable choice by noting that “string breaking” should occur when the energy of the extended string is equal to the energy of

the lowest two-meson state that can be formed when the string breaks. Therefore, we may write $V_{max} = m_1 + m_2$, where $m_1 + m_2$ are the masses of the mesons in the final state. We then use $V_{max} = \kappa/\mu(\rho)e$ to find a value $\mu(\rho)$ and obtain ρ/ρ_C from the expression $\mu(\rho) = \mu_0/[1 - (\rho/\rho_C)^2]$. We then put $\rho_C = 2.25\rho_{NM}$ and calculate the value of ρ/ρ_{NM} where we might expect string breaking. We consider the final states $\pi\pi$, πK , $\pi\eta$ and $K\bar{K}$. The corresponding values of ρ/ρ_{NM} are 2.09, 1.86, 1.83, and 1.61 for $\rho_C = 2.25\rho_{NM}$. Note that the $K(495)$ and $K_0^*(1430)$ mesons can break up into the πK system, while the $a_0(980)$ is strongly coupled to the $\pi\eta$ channel. The $f_0(980)$ is coupled both to the $\pi\pi$ and $K\bar{K}$ channels. On the whole, the values of ρ/ρ_{NM} calculated above are generally consistent with the value of that quantity that leads to deconfinement in our model. That result tends to suggest that, for light mesons, the density that leads to string breaking may be similar to the density for deconfinement. (In general, however, these processes are distinct and further studies would be needed to see if string breaking and deconfinement are related at finite density.) We may suggest that, if the initial meson is of the same type as the mesons that appear upon string breaking, it becomes reasonable to suggest that the instability of the initial mesons is also felt by the final state mesons, giving rise to the relation of string breaking and deconfinement suggested above for light mesons.

A comprehensive discussion of meson properties at finite temperature and density has been presented by Lutz, Klimt and Weise [32]. Since those authors did not include a model of confinement, they were able to calculate values of the meson masses for large values of the density. Their Fig. 8 shows the calculated masses of the nodeless pion, f_0 and a_0 mesons for $0 \leq \rho/\rho_{NM} \leq 3.5$. They also give the result for an f'_0 excitation. (The f_0 and f'_0 exhibit singlet-octet mixing.) Compared to our results, their value of the f_0 mass falls more rapidly than ours, becoming degenerate with the pion mass at about $\rho/\rho_{NM} = 3$. On the other hand, the mass of the a_0 in their work is about 600 MeV at $\rho/\rho_{NM} = 2$. They are able to derive systematic low-density expansions for various quantities which provide important insight into the results obtained in numerical studies. They also show that effects due to finite quasiparticle size are important in stabilizing the density and temperature dependence of the pion mass. The main deficiency of their work is the absence of a model of confinement. Therefore, we believe our work provides a natural extension of the work reported in Ref. [32].

It is worth noting that deconfinement takes place in our model at about $\rho = 1.8\rho_{NM}$,

while the confining potential goes to zero at $\rho = \rho_C = 2.25\rho_{NM}$. That suggests that the specific form we have chosen for the density dependence, $\mu(\rho) = \mu_0/[1 - (\rho/\rho_C)^2]$, is not particularly important. What is more important is the behavior of our confining potential, $V^C(r, \rho)$, shown in Fig. 5. There, we see that the potential still has a substantial magnitude at $\rho = 1.75\rho_{NM}$ and $\rho = 2.10\rho_{NM}$.

Since the analysis of Ref. [32] is made in the absence of a model of confinement, many analytic results can be obtained for the behavior of various quantities when small changes in density and temperature are considered. Indeed, the work of that reference provides some support for our treatment of the pion and kaon. It is shown that the Goldstone boson remains at zero mass in the chiral limit as long as the system remains in the Goldstone-Nambu mode of symmetry breaking. For finite current quark masses, we quote the result given in Eq. (5.6) of Ref. [32] for $T = 0$,

$$\frac{dm_\pi^2}{m_\pi^2} = (1 - 2m_u^2 \langle r_S^2 \rangle) \frac{d\langle \bar{u}u \rangle}{\langle \bar{u}u \rangle}. \quad (9.1)$$

Here, r_S is the quasiparticle radius. That quantity is defined in terms of the form factor $F_S(\vec{p} - \vec{p}')$ that appears in the matrix element of the u-quark scalar density

$$\langle u(\vec{p}') | \bar{u}u(0) | u(\vec{p}) \rangle = F_S(\vec{p} - \vec{p}') \bar{u}(p') u(p). \quad (9.2)$$

In Eq. (9.2) $u(\vec{p})$ denotes the Dirac spinor of a constituent u quark with four-momentum p . The scalar mean-squared radius is then

$$\langle r_S^2 \rangle = 6 \frac{d}{dq^2} \ln F_S(q^2) \Big|_{q^2=0}. \quad (9.3)$$

(See Eq. (A.7) of Ref. [32] for an explicit expression for $\langle r_S^2 \rangle$ in terms of the parameters of the NJL model.) With the well-known relation [20]

$$\frac{d\langle \bar{u}u \rangle}{\langle \bar{u}u \rangle} = - \frac{\sigma_N \rho}{m_\pi^2 f_\pi^2}, \quad (9.4)$$

Eq. (9.1) becomes

$$dm_\pi^2 = - (1 - 2m_u^2 \langle r_S^2 \rangle) \frac{\sigma_N \rho}{f_\pi^2}. \quad (9.5)$$

If one ignores the quasiparticle size, one has $dm_\pi^2 = -(\sigma_N \rho / f_\pi^2)$ [33, 34], which implies pion condensation at a critical density $\rho_{crit} = f_\pi^2 m_\pi^2 / \sigma_N = (0.148 \text{ GeV})^3$, which is about 2.5 ρ_{NM} .

The second term in Eq. (9.5) works against condensation. With $m_u = 0.364$ GeV and $r_S = 0.40$ fm [32] one finds that δm_π^2 increases slowly with increasing density, as born out by the calculations reported in Ref. [32]. Our choice of $G_\pi(\rho) = G_\pi(0)[1 - 0.087\rho/\rho_{NM}]$ reproduces the almost constant value of m_π . We see that the density-dependent term in $G_\pi(\rho)$ plays a similar role in our model as that played by the second term in Eq. (9.5).

We have some confidence in our treatment of the pion and kaon at finite density. We recall that we were able to find satisfactory values of $G_\pi(0)$ and $G_K(0)$ using the values of G_S and G_D obtained in our study of the eta mesons [1]. Therefore, our work provides a unified approach for the nonet of pseudoscalar mesons in the presence of a model of confinement.

Since confinement is important for the $a_0(980)$ and $f_0(980)$ mesons, it is uncertain whether the results of Ref. [32] for the properties of these mesons can be trusted. These mesons are in the continuum of the NJL model without confinement and various assumptions need to be made as to how the formalism is to be applied. For a small increase in density, the mass of the a_0 in our model and in Ref. [32] are similar. For the larger values of density, the use of $G_{a_0}(\rho) = G_{a_0}(0)[1 - 0.045\rho/\rho_{NM}]$ in model leads to a rather small mass for the a_0 for $\rho \sim 2\rho_{NM}$. [See Fig. 8.]

Our treatment of the a_0 mesons is less satisfactory than that of π and K mesons, since coupled channel effects are important in the case of the scalar mesons. Using the values of G_S and G_D obtained in our study of the eta mesons [1], we found the lowest a_0 state at 1.13 GeV. To place the a_0 at 980 MeV, we increased the value of $G_{a_0}(0)$. That increase led to the possibility of an a_0 condensation, which was removed by reducing the coupling constant with increasing density. [See Fig. 8.] However, it might be preferable to accept the value of 1.13 GeV for the mass of the a_0 and, therefore, avoid the problem of a_0 condensation. Our difficulty in this case arises since we do not know the density dependence of the processes that move the a_0 mass from our predicted value to the experimental value of 980 MeV.

In our model we see some relation between the partial restoration of chiral symmetry and deconfinement. With reference to Fig. 2, we see that the up (or down) quark mass drops in a roughly linear manner with increasing density up to about 2 or 2.5 times nuclear matter density. With the reduction of the magnitude of the confining field, as seen in Fig. 5, the combined effect of the smaller confining field and reduced quark mass values leads to deconfinement at about $1.8 \rho_{NM}$. For the f_0 , K and K_0^* mesons, the reduction of the mass of the quarks is less important, since these mesons have either one strange quark (K , K_0^*)

or an $\bar{s}s$ component (f_0). However, deconfinement still takes place at about $\rho = 1.8\rho_{NM}$ for the mesons.

In future work we will study the dependence of the deconfinement process on both temperature and density. In addition, it would be desirable to have some understanding of the mechanism by which the increased matter density modifies the confining interaction.

References

- [1] C. M. Shakin and Huangsheng Wang, Phys. Rev. D **65**, 094003 (2002).
- [2] C. M. Shakin and Huangsheng Wang, Phys. Rev. D **64**, 094020 (2001).
- [3] C. M. Shakin and Huangsheng Wang, Phys. Rev. D **63**, 074017 (2001).
- [4] L. S. Celenza, Huangsheng Wang, and C. M. Shakin, Phys. Rev. C **63**, 025209 (2001).
- [5] C. M. Shakin and Huangsheng Wang, Phys. Rev. D **63**, 014019 (2000).
- [6] For reviews, see K. Rajagopal and F. Wilcek, in B. L. Ioffe Festschrift; *At the Frontier of Particle Physics/Handbook of QCD*, M. Shifman ed. (World Scientific, Singapore 2001); M. Alford, hep-ph/0102047.
- [7] M. Alford, R. Rajagopal and F. Wilcek, Phys. Lett. B **422**, 247 (1998).
- [8] R. Rapp, T. Schäfer, E. V. Shuryak and M. Velkovsky, Phys. Rev. Lett. **81**, 53 (1998).
- [9] M. Alford, J. Berges and K. Rajagopal, Nucl. Phys. B **558**, 219 (1999).
- [10] S. P. Klevansky, Rev. Mod. Phys. **64**, 649 (1992).
- [11] U. Vogl and W. Weise, Prog. Part. Nucl. Phys. **27**, 195 (1991).
- [12] T. Hatsuda and T. Kunihiro, Phys. Rep. **247**, 221 (1994).
- [13] C. DeTar, O. Kaczmarek, F. Karsch, and E. Laermann, Phys. Rev. D **59**, 031501 (1998).
- [14] C. D. Roberts and S. M. Schmidt, Prog. Part. Nucl. Phys. **45**, S1 (2000).
- [15] C. Shakin, Ann. Phys. (NY) **192**, 254 (1989).
- [16] L. S. Celenza, Hui-Wen Wang and Xin-Hua Yang, Intl. J. Mod. Phys. A **4**, 3807 (1989).
- [17] V. M. Bannur, L. S. Celenza, Huang-he Chen, Shun-fu Gao and C. M. Shakin, Intl. J. Mod. Phys. A **5**, 1479 (1990).
- [18] V. M. Bannur, L. S. Celenza, C. M. Shakin, and Hui-Wen Wang, Description of the QCD Vacuum as a Random Medium, Brookly College Report: BCCNT89/032/189—unpublished.

- [19] L. S. Celenza, Bing He, Hu Li, Qing Sun, and C. M. Shakin, nucl-th/0203010.
- [20] E. G. Drukarev and E. M. Levin, Prog. Part. Nucl. Phys. **27**, 77 (1991).
- [21] B. D. Serot and J. D. Walecka, in Advances in Nuclear Physics, Vol. 16, edited by J. W. Negele and E. Vogt (Plenum, New York, 1986).
- [22] L. S. Celenza and C. M. Shakin, *Relativistic Nuclear Physics: Theories of Structure and Scattering* (World Scientific, Singapore, 1986).
- [23] Nan-Wei Cao, C. M. Shakin and Wei-Dong Sun, Phys. Rev. C **46**, 2535 (1992).
- [24] C. Bernard *et al.*, Phys. Rev. D **64**, 074509 (2001).
- [25] A. B. Migdal, Soviet Phys., JETP **34**, 1184 (1972).
- [26] T. Ericson and W. Weise, *Pions and Nuclei* (Oxford Univ. Press, Oxford, 1988).
- [27] L. S. Celenza, Shun-fu Gao, Bo Huang, Huangsheng Wang, and C. M. Shakin, Phys. Rev. C **61**, 035201 (2000).
- [28] C. M. Shakin, Phys. Rev. D **65**, 114011 (2002).
- [29] A. L. Fetter and J. D. Walecka, *Quantum Theory of Many-Particle Systems*, (Mc Graw-Hill, New York, 1971).
- [30] D. J. Rowe, *Nuclear Collective Motion*, (Methuen, London, 1970).
- [31] C. M. Shakin and Huangsheng Wang, Phys. Rev. D **63**, 114007 (2001).
- [32] M. Lutz, S. Klimt, and W. Weise, Nucl. Phys. A **541**, 521 (1992).
- [33] D. B. Kaplan and A. E. Nelson, Phys. Letter. B **175**, 57 (1986).
- [34] A. E. Nelson and D. B. Kaplan, Phys. Letter. B **192**, 193 (1987).